The structures of chiral and racemate campho[2,3- c]pyrazole: A combined crystallographic, solid-state NMR and computational study

ARTICLE *in* JOURNAL OF MOLECULAR STRUCTURE · FEBRUARY 2010

Impact Factor: 1.6 · DOI: 10.1016/j.molstruc.2009.11.041

Journal of Molecular Structure 965 (2010) 74–81

Contents lists available at ScienceDirect

Journal of Molecular Structure

journal homepage: www.elsevier.com/locate/molstruc

The structures of chiral and racemate campho[2,3-*c*]pyrazole: A combined crystallographic, solid-state NMR and computational study

Glenn P.A. Yap [a], Rosa M. Claramunt [b], Concepción López [b], M. Ángeles García [b], Carlos Pérez-Medina [b], Ibon Alkorta [c,*], José Elguero [c]

[a] Department of Chemistry and Biochemistry, University of Delaware, Newark, DE 19716, USA
[b] Departamento de Química Orgánica y Bio-Orgánica, Facultad de Ciencias, UNED, Senda del Rey 9, E-28040 Madrid, Spain
[c] Instituto de Química Médica, CSIC, Juan de la Cierva 3, E-28006 Madrid, Spain

ARTICLE INFO

Article history:
Received 28 September 2009
Received in revised form 11 November 2009
Accepted 13 November 2009
Available online 22 November 2009

This paper is dedicated to Professor Robert Jacquier who passed away in January 2009

Keywords:
Pyrazole
Crystallography
CPMAS NMR
GIAO
$Z' = 6$

ABSTRACT

Crystallographic and solid CPMAS NMR studies were performed on the (4*S*,7*R*)-enantiomer as well as on the (4*S*,7*R*)- and (4*R*,7*S*)-7,8,8-trimethyl-4,5,6,7-tetrahydro-4,7-methano-2*H*-indazole racemate. Both crystallize with six independent molecules forming two trimers. Assignment of the ^{13}C chemical shifts to the six molecules, slighting differing in geometry, was carried out by comparison with GIAO/B3LYP/6-31G(d) calculations.

1. Introduction

Campho[2,3-*c*]pyrazole [(4*S*,7*R*)-7,8,8-trimethyl-4,5,6,7-tetrahydro-4,7-methano-2*H*-indazole] is prepared from camphor in a classical two-step procedure (Scheme 1). It was first synthesized by Wallach in 1903 [1] and then by Finnish authors in 1944 [2] but, because of the obscurity of the original literature, it is the Jacquier and Maury 1967 procedure [3] that is commonly cited by subsequent authors. This compound was always prepared from natural camphor so it is the (4*S*,7*R*) enantiomer **1** that was obtained.

2. Results and discussion

Campho[2,3-*c*]pyrazole (**1**) has been the subject of many studies: synthetic [4–6], structural [7], reactivity [3,8–12], and as ligands in coordination chemistry [13–19]. The tautomerism has been studied proving that the proton is at the 2-position (2*H*-indazole) [7,20], a fact that has been related to the Mills-Nixon effect [21].

In the solid-state campho[2,3-*c*]pyrazole (**1**) has two very interesting properties (refcode LABHEB [22]): (i) there are six independent molecules in the unit cell ($Z' = 6$) and (ii) due to its globular shape the ^{13}C NMR spectrum is very well resolved (Fig. 1 [7]) and several of its carbon atoms show up to six different signals, one for each independent molecule [7,23,24]. There is a great interest in structures containing a large number of independent molecules [25–27] of which **1** is a clear representative. Compound **1** crystallizes forming two cyclic trimers (cyclamers), trimers being a common motif in NH-pyrazoles [28,29] (Scheme 2 and Fig. 2).

Note that no structural study of the (**1** + **2**) racemate has ever been reported.

2.1. Solution studies

The ^{13}C NMR spectra in solution ($CDCl_3$) of both, chiral **1** and **2** as well as racemic (**1** + **2**) campho[2,3-*c*]pyrazole mixture, are identical. The experimental chemical shifts (δ, ppm) and absolute shieldings (σ, ppm) [GIAO/B3LYP/6-31G(d) calculations] are linearly related (Eq. (1)): C3 (119.84/78.18), C3a (125.72/69.01), C4 (47.06/137.25), C5 (27.79/158.92), C6 (33.68/153.63), C7 (49.91/140.80), C7a (165.77/32.41), C8 (60.99/126.26), 7Me (10.83/176.11), $8Me_{syn}$ (20.43/168.20) and $8Me_{anti}$ (19.23/169.13). The trendline equation is

* Corresponding author. Tel.: +34 91 562 29 00; fax: +34 91 564 48 53.
E-mail address: ibon@iqm.csic.es (I. Alkorta).

0022-2860/$ - see front matter © 2009 Elsevier B.V. All rights reserved.
doi:10.1016/j.molstruc.2009.11.041

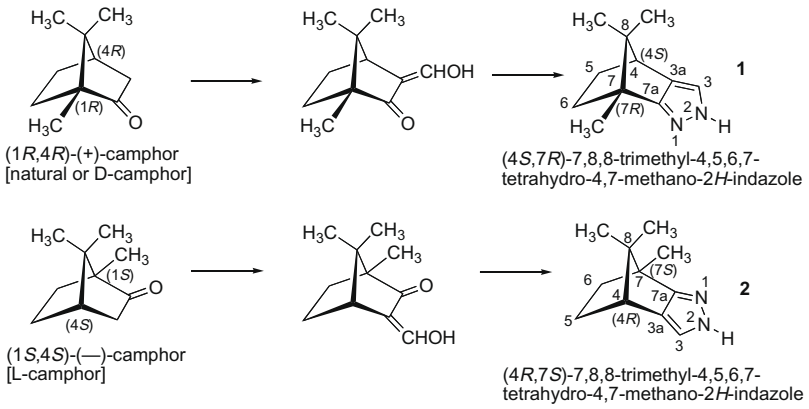

Scheme 1. The two enantiomers of campho[2,3-*c*]pyrazole.

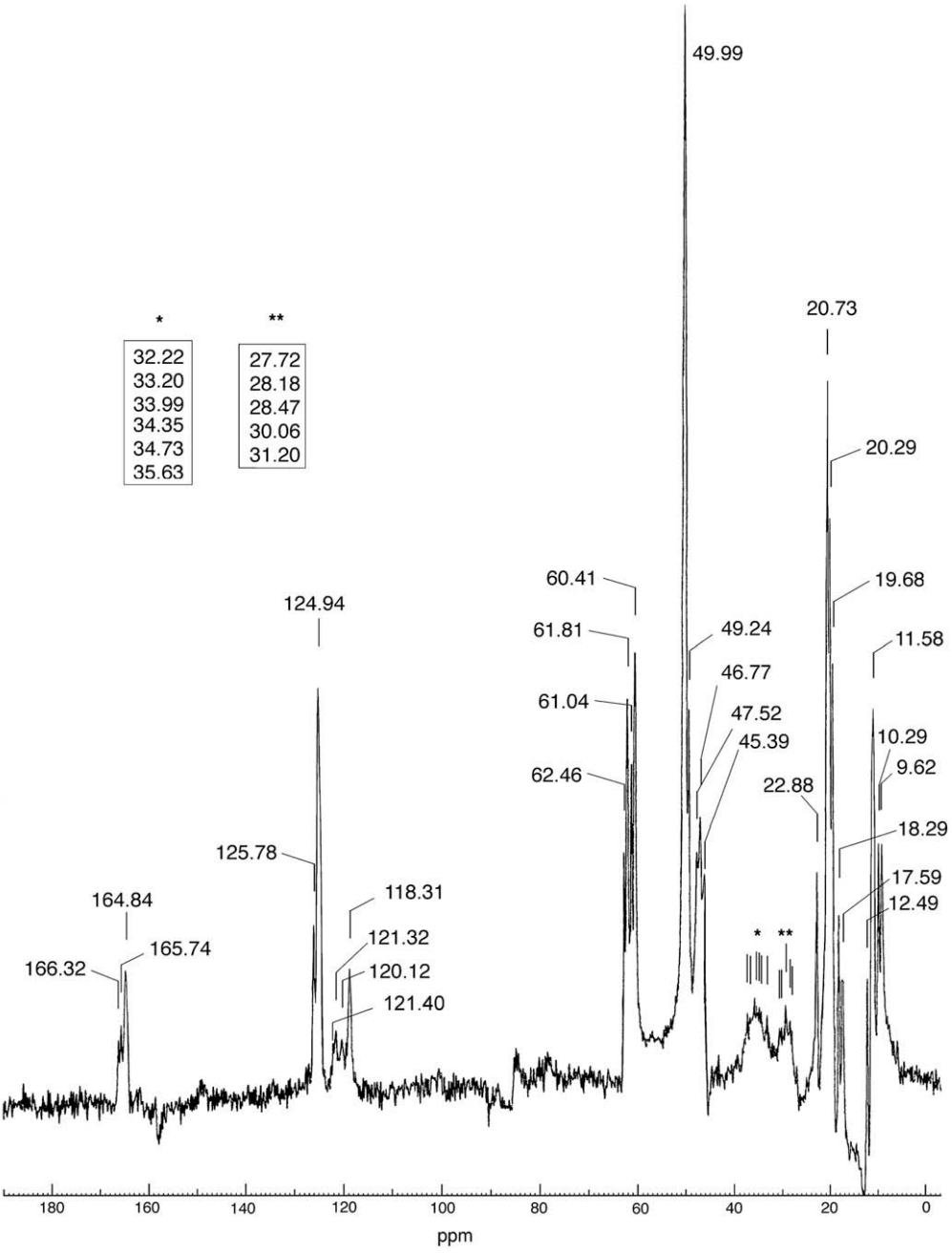

Fig. 1. The 100.63 MHz ^{13}C CPMAS NMR spectrum of **1** [7].

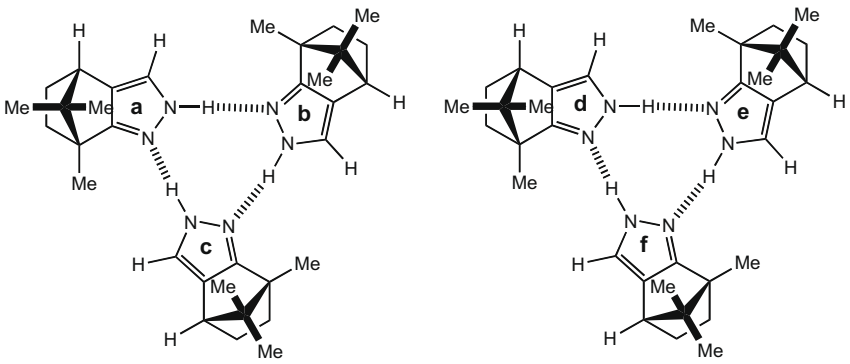

Scheme 2. The six independent molecules (**a**–**f**) forming two trimers, the first one formed by **a**, **b** and **c** monomers and the second one by **d**, **e** and **f** monomers.

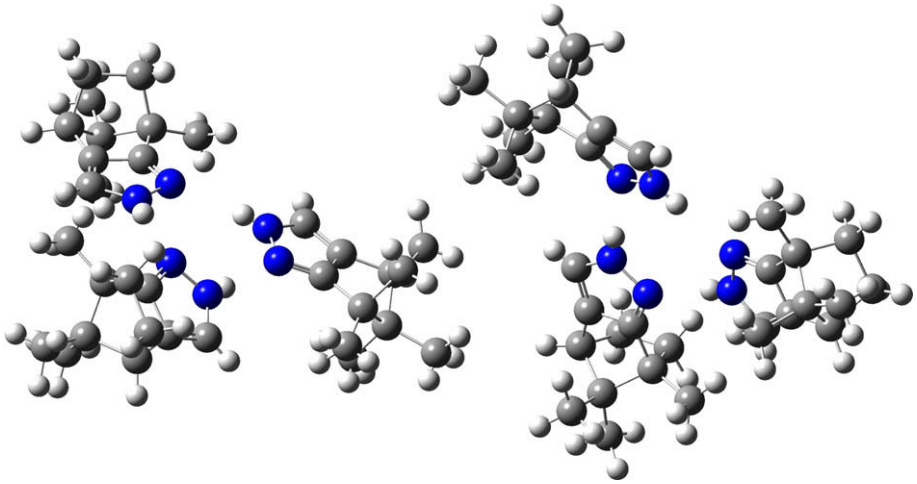

Fig. 2. The two crystallographic trimers of **1** (LABHEB).

$$\delta^{13}\mathrm{C(ppm)} = (201.11 \pm 2.32) - (1.086 \pm 0.017)\sigma^{13}\mathrm{C(ppm)},\quad n = 11, R^2 = 0.9978 \qquad (1)$$

Eq. (1) is similar to that described previously by us also for GIAO/B3LYP/6-31G(d) calculations: $\delta^{13}C = 203.0–1.086\ \sigma^{13}C$ [30].

2.2. Solid-state studies: chiral compound

Compound **1** is one of the compounds that yielded a very well resolved ^{13}C CPMAS NMR spectrum (see Fig. 1). Perfect resolution will lead to six signals for each one of the eleven carbon atoms. This is not always the case but when several signals coincide, the intensity is proportional to the number of identical chemical shifts. We have gathered in Table 1 the values obtained in our previous paper at 100.63 Hz [7]) and the calculated absolute shieldings. We recorded again the ^{13}C CPMAS NMR spectrum at the same frequency obtaining an almost identical spectrum (Fig. 3). The assignment of all signals to the corresponding carbon atoms is straightforward save those of $8Me_{anti}$ and $8Me_{syn}$, which were assigned using the calculated absolute shieldings.

The ^{15}N CPMAS NMR spectrum of **1** shows only two signals at −107.4 (N1) and −177.2 ppm (N2) (Fig. 4a). There is no splitting due to the existence of six different molecules in the asymmetric unit, although according to the calculations there is a span of 4–5 ppm between the different signals. The reason is that in natural abundance each ^{15}N is linked to a ^{14}N.

The GIAO/B3LYP/6-31G(d) calculations correspond to the following situations: (i) for solution (see above) the fully optimized [(B3LYP/6-31G(d)] geometry was used; (ii) for the solid state, the six experimental geometries of LABHEB were used with the non-hydrogen atoms (C and N) in their crystallographic positions while the H atoms were optimized. The optimization of the position of H atoms is crucial, otherwise the calculated ^{13}C shieldings were very different from those that correspond to the experimental values. The requirement to optimize the positions of the H atoms is undoubtedly due to the fact that the hydrogen positions determined by X-ray always have C–H bond lengths shorter (*ca.* 10%) than the real internuclear distances.

When there is no problem to assign each group of signals to a particular carbon atom, we have assigned the signal of a determined C atom to the calculated molecule in order to have the best fit. To verify this assumption it would be necessary to establish the connectivity between linked carbon atoms for each independent molecule using the INADEQUATE sequence [31].

The results are reported in Table 1.

The trendlines are:

$$\delta^{13}\mathrm{C}[7] = (204.1 \pm 0.8) - (1.091 \pm 0.006)\sigma^{13}C,\quad n = 66, R^2 = 0.9980 \qquad (2)$$

$$\delta^{13}\mathrm{C(this\ work)} = (204.2 \pm 0.8) - (1.093 \pm 0.006)\sigma^{13}\mathrm{C},\quad n = 66, R^2 = 0.9980 \qquad (3)$$

Worse points correspond to C3 of **e** (+7.9 ppm) and C7a of **a** (−4.0 ppm).

Table 1
^{13}C chemical shifts (δ in ppm) and absolute shieldings (σ, in ppm) of (4*S*,7*R*)-7,8,8-trimethyl-4,5,6,7-tetrahydro-4,7-methano-2*H*-indazole (**1**).

Molecule	Carbon atom	From Ref [7]	This work	σ Monomer	σ Trimer
First trimer:					
a	C3	120.12	120.11	79.86	80.20
	C3a	125.78	125.78	71.21	72.23
	C4	47.52	47.56	141.18	142.45
	C5	28.47	27.64	160.26	161.43
	C6	34.35	34.32	155.02	155.05
	C7	49.99	49.96	139.47	140.65
	C7a	166.32	166.30	30.97	31.61
	C8	62.46	62.36	127.81	127.43
	7Me	11.58	11.47	176.30	176.21
	8Me$_{anti}$	17.59	17.62	169.13	169.52
	8Me$_{syn}$	20.73	20.70	167.78	168.69
b	C3	118.31	118.27	81.17	81.19
	C3a	124.94	124.91	71.55	74.31
	C4	46.77	46.84	142.31	142.44
	C5	30.06	28.14	160.28	160.82
	C6	35.63	35.66	155.19	154.94
	C7	49.99	49.96	140.10	140.91
	C7a	164.84	164.79	33.41	35.32
	C8	60.41	60.35	133.62	132.82
	7Me	9.62	9.57	176.32	177.27
	8Me$_{anti}$	20.29	20.23	169.23	169.20
	8Me$_{syn}$	20.73	20.70	168.24	168.19
c	C3	118.31	118.27	82.58	80.47
	C3a	124.94	124.91	72.63	73.72
	C4	46.77	46.84	142.60	142.69
	C5	28.18	46.84	161.59	161.44
	C6	33.99	32.99	156.43	155.34
	C7	49.99	49.96	140.63	140.35
	C7a	164.84	164.79	34.62	34.72
	C8	60.41	60.35	132.07	131.44
	7Me	11.58	11.47	176.86	176.52
	8Me$_{anti}$	19.68	19.65	169.60	169.27
	8Me$_{syn}$	20.73	20.70	169.06	169.03
Second trimer:					
d	C3	118.31	118.27	81.96	80.48
	C3a	124.94	124.91	71.82	72.53
	C4	46.77	46.84	142.34	142.86
	C5	27.72	26.77	160.87	161.92
	C6	32.22	31.69	155.32	156.66
	C7	49.99	49.96	140.58	140.83
	C7a	165.74	165.72	33.47	34.40
	C8	61.81	61.75	129.45	128.99
	7Me	10.29	10.22	175.52	176.73
	8Me$_{anti}$	20.23	20.23	169.29	169.11
	8Me$_{syn}$	20.23	22.77	168.73	169.25
e	C3	121.32	121.45	83.13	78.68
	C3a	125.78	125.78	73.37	72.01
	C4	45.39	46.44	143.55	143.42
	C5	30.06	28.14	161.93	160.32
	C6	34.73	34.70	156.66	155.02
	C7	49.24	49.23	140.75	140.91
	C7a	164.84	164.79	34.85	35.55
	C8	61.81	61.75	128.64	128.41
	7Me	11.58	11.47	177.69	176.06
	8Me$_{anti}$	18.29	18.33	169.65	169.51
	8Me$_{syn}$	22.88	22.91	169.09	168.02
f	C3	121.40	121.60	82.53	78.04
	C3a	124.94	124.91	72.59	73.37
	C4	47.52	47.56	142.46	141.08
	C5	31.20	29.17	161.08	160.11
	C6	32.22	32.71	155.33	156.59
	C7	49.99	49.96	140.59	139.60
	C7a	164.84	164.79	34.11	36.03
	C8	61.04	61.03	131.38	130.69
	7Me	12.49	12.39	176.52	175.57
	8Me$_{anti}$	20.73	20.70	169.35	168.92
	8Me$_{syn}$	19.68	19.65	169.03	169.30

Then we calculated trimers (Scheme 2) instead of isolated monomers. The largest differences between σ values of isolated monomers and monomers within trimers are +3.4 ppm (C3 of **a**) and −3.5 ppm (C7a of **a**).

$$\delta^{13}\mathrm{C}[7] = (204.5 \pm 0.5) - (1.094 \pm 0.004)\sigma^{13}\mathrm{C}, \quad n = 66, R^2 = 0.9992 \tag{4}$$

$$\delta^{13}\mathrm{C}(\text{this work}) = (204.6 \pm 0.5) - (1.096 \pm 0.004)\sigma^{13}\mathrm{C}, \quad n = 66, R^2 = 0.9993 \tag{5}$$

Worse points correspond to C3 of **a** (+3.4 ppm) and C7a of **a** (−3.6 ppm).

The calculations leading to Eqs. (4) and (5) identify molecules within each trimer. Calculations based on trimers improve the correlation but C3 and C7a continue to be the atoms with the largest residuals, probably because they are linked to ^{14}N atoms. A model using dummy variables for C3 and C7a lead to Eq. (6).

$$\delta^{13}\mathrm{C}[7] = (204.1 \pm 0.7) - (1.093 \pm 0.005)\sigma^{13}\mathrm{C} + (2.8 \pm 0.6)\mathrm{C3} - (1.3 \pm 0.7)\mathrm{C7a}, \quad n = 66, R^2 = 0.9995 \tag{6}$$

$$\delta^{13}\mathrm{C}(\text{this work}) = (204.3 \pm 0.6) - (1.095 \pm 0.004)\sigma^{13}\mathrm{C} + (2.7 \pm 0.5)\mathrm{C3} - (1.5 \pm 0.7)\mathrm{C7a}, \quad n = 66, R^2 = 0.9996 \tag{7}$$

Eqs. (6) and (7) mean that the calculations underestimated C3 carbon atoms by 2.7–2.8 ppm on average and overestimated C7a carbon atoms by 1.3–1.5 ppm in average (worse points C4 of **f** and Me$_{syn}$ of **e**, both less than 2.5 ppm).

2.3. Solid-state studies: racemate

It was difficult to grow crystals of the racemate to carry out a X-ray crystal structure determination. The racemate consistently deposited as multiple, small, weakly diffracting crystals. Using the best data crystal available, we obtained the following data and we compared them with those of LABHEB (Table 2).

If there is no spontaneous resolution, the crystals of the racemate compound should correspond to situations like **I** or **II** (Fig. 5). Spontaneous partial resolution will lead to crystals of type **III**, some of them rich in enantiomer **1** (**IIIa**) and others in enantiomer **2** (**IIIb**). Many other situations are possible including very complex mixtures. The crystal whose structure has been solved predominantly corresponds to **IIIa** (wherein there are five molecules of **1** and one molecule of **2**) with a minor enantiopure component of **1** (Fig. 6).

Note that assignment of absolute configuration based solely on X-ray in the absence of heavy atoms is generally considered unwise but the diagrams show the configuration that seems favored by the data. If the chiral center with the methyl is 7 then the predominant enantiomer in this specific crystal is 4*S*,7*R* (**1**). Apparently the trimers are dictated only by the H-bonding and inverting one camphor ring is allowed to form the minor 4*S*–4*S*–4*R* trimer. Presumably, a whole range of possible racemic distributions could be formed. Perhaps this would explain why it has been somewhat difficult to generate good quality crystals since there were several possible crystal phases. A purely 50/50 racemate crystal could have a centrosymmetric space group such as $P2_1/m$, for example, while maintaining similar unit cell parameters.

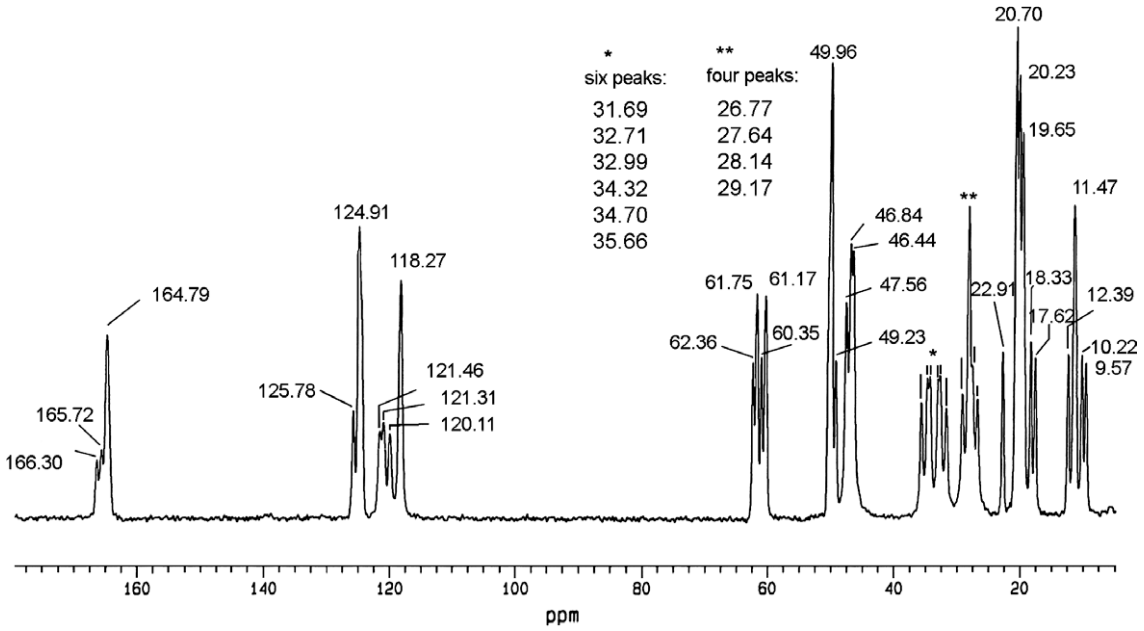

Fig. 3. The 100.73 MHz ^{13}C CPMAS NMR spectrum of **1**.

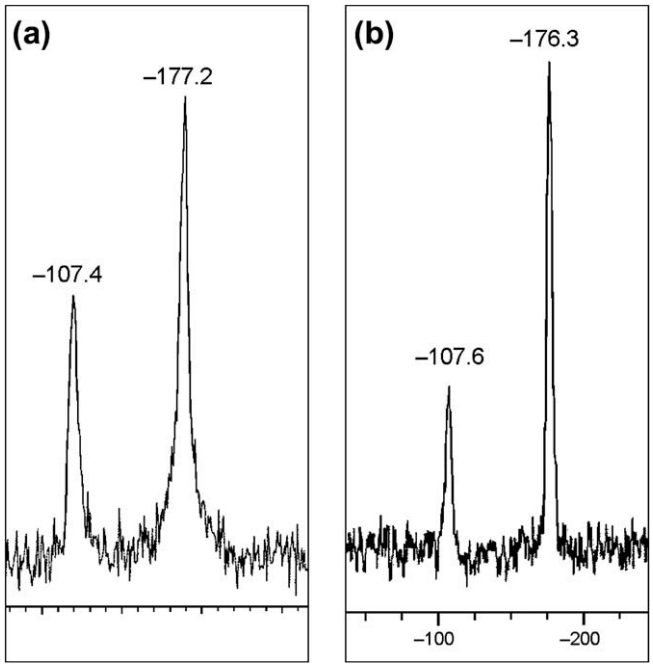

Fig. 4. The 40.6 MHz ^{15}N CPMAS NMR spectra of (a) **1** and (b) **1** + **2**.

The ^{13}C CPMAS NMR spectrum of the racemate is reported in Fig. 7 and the ^{15}N CPMAS NMR spectra of enantiomer **1** and racemate **1** + **2** in Fig. 4. The ^{15}N NMR spectra are very similar but the ^{13}C of the racemate has lower resolution, an indication of its static disorder. Although in the crystal we have determined there is an excess of the 4*S* enantiomer (the natural one **1**), in the batch there should be an equal number of **1** and **2** enantiomers because we measured the optical rotatory power in chloroform of **1** (α = +0.060°, $[\alpha]^{25}_D$ = + 24°, *c* = 0.25 g/100 mL) and **1** + **2** (α = −0.003°, $[\alpha]^{25}_D$ = −1°, *c* = 0.31 g/100 mL). It is interesting to note that the melting point of enantiomer **1** determined by DSC is 152.9 °C (lit-

Table 2
Crystallographic comparison between (**1** + **2**) racemate and enantiopure (LABHEB, LABHEB01) campho[2,3-*c*]pyrazole.

	1 + **2**[1]	LABHEB [7]	LABHEB01 [32]
Crystal system	Monoclinic	Monoclinic	Monoclinic
Space group	$P2_1$	$P2_1$	$P2_1$
Temperature (K)	120(2)	283–303	150
a (Å)	13.313(2)	13.408(<1)	13.264(<1)
b (Å)	12.484(2)	12.606(<1)	12.490(<1)
c (Å)	18.686(3)	19.052(<1)	18.854(<1)
β (°)	97.932(3)	98.39(<1)	98.25(<1)
V (Å^3)	3075.7(9)	3185.793	3091.231
Z, *Z*′	12, 6	12, 6	12, 6
D_{calc} (g/cm^3)	1.142	1.102	1.136
Reflections collected/ unique	27223/7111	NA	NA
Completeness to θ = 25° (%)	99.9	NA	NA
Data/restraints/parameters	7111/42/758	NA	NA
Goodness of fit on F^2	1.067	NA	NA
R, wR^2 ($I > 2\sigma$)	0.0570, 0.1475	0.057	0.0523
R, wR^2 (all data)	0.0592, 0.1494	NA	NA
Deposition	CCDC 747613	IUCr AL1008	CCDC 660835

[1] quantity minimized = $\Sigma w(F_o^2 - F_c^2)^2$.

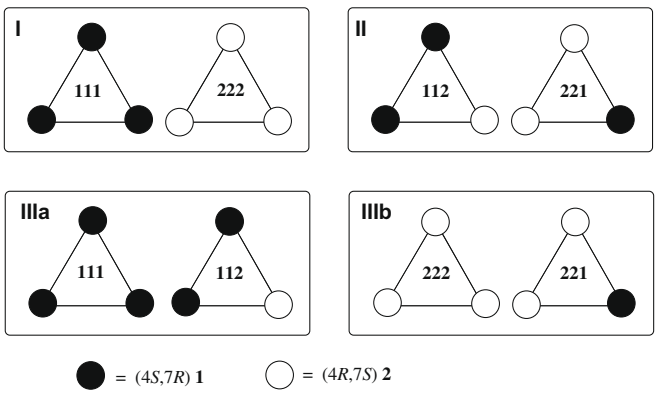

Fig. 5. The possible double trimers of the racemic campho[2,3-*c*]pyrazole (**1** + **2**) mixture.

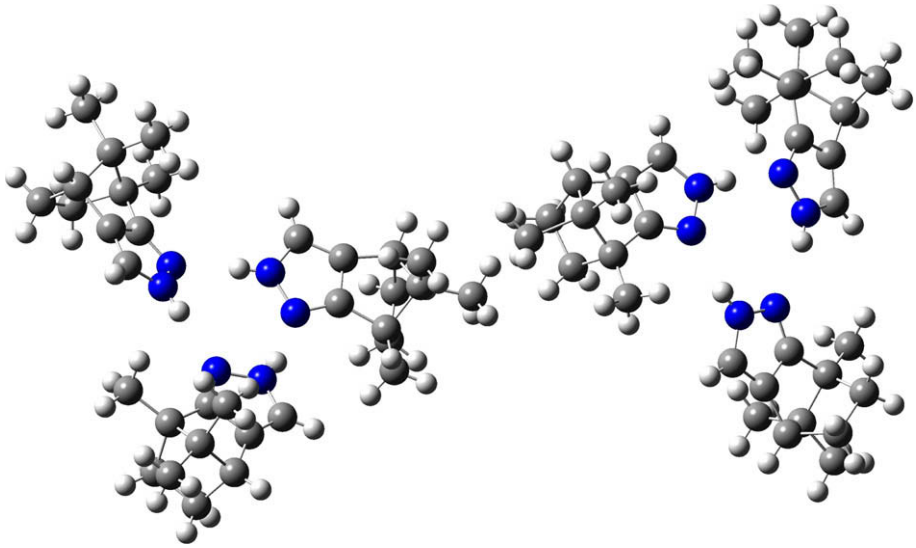

Fig. 6. The two crystallographic trimers of **1** + **2**.

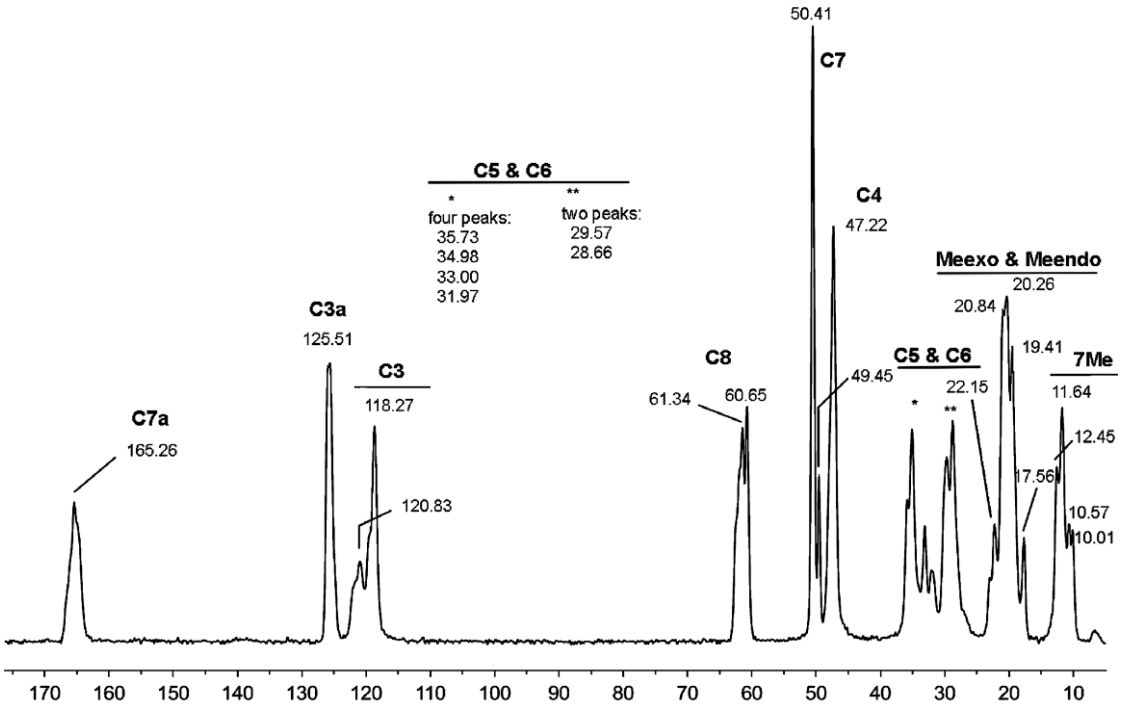

Fig. 7. The 100.73 MHz ^{13}C CPMAS NMR spectrum of **1** + **2**.

erature 137–138 °C [3] and 143–144 °C [2]) while that of the racemate **1** + **2** is 139.1 °C [33].

We have calculated the GIAO absolute shieldings of the trimer of Fig. 8 using the same procedure as for the chiral compound (non-hydrogen atoms from the X-ray structure and optimizing the H atoms at the 6-31G* level) and reported them together with the calculated and experimental δ values in Table 3.

The last column of Table 3 does not correspond exclusively to the 4*S*(**g**)–4*S*(**h**)–4*R*(**i**) trimer (**112**) but to all trimers including the 4*S*–4*S*–4*S* (**111**) present in the unit cell (see Fig. 5). The calculations only show that the presence of the **ghi** trimer is compatible with the experimental data.

3. Conclusions

Chiral campho[2,3-*c*]pyrazole (**1**) is still a fascinating molecule that will continue to be used in chemistry and studied *per se*. The present work provides an explanation to the behavior of **1** in the solid state. To go further, $^{15}N_2$-labeling, high-field apparatus and connectivity NMR techniques would be necessary.

Racemic campho[2,3-*c*]pyrazole mixture (**1** + **2**) has been studied here for the first time showing interesting structural features. Since **111** and **112** trimers have similar energies [0.03 kJ mol^{-1} at the B3LYP/6-31G(d) level and 0.40 kJ mol^{-1} at the B3LYP/6-31+G(d,p) level the **111** being the most stable] (**222** and **221** tri-

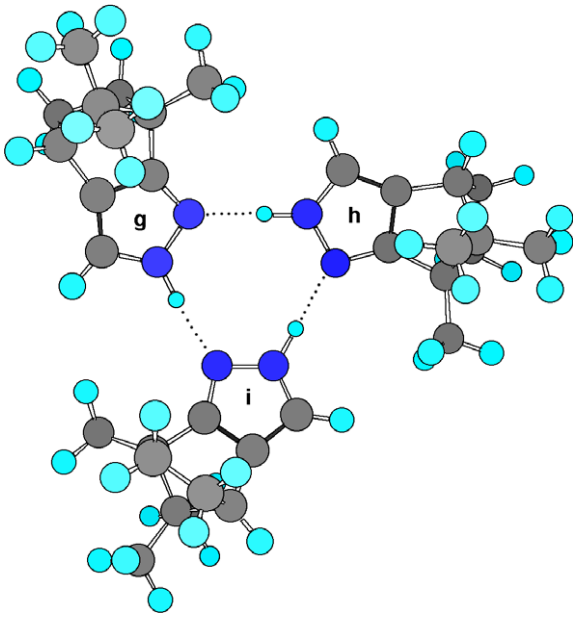

Fig. 8. The 4*S*(**g**)–4*S*(**h**)–4*R*(**i**) trimer of **1** + **2**.

mers are enantiomers of the preceding ones) the crystal structure is formed by unit cells containing both types of trimers. This compound should be a good candidate for total spontaneous resolution under different conditions.

Table 3
^{13}C absolute shieldings (σ, in ppm) and chemical shifts (δ in ppm) of racemic 7,8,8-trimethyl-4,5,6,7-tetrahydro-4,7-methano-2*H*-indazole mixture (**1** + **2**). To transform σ into δ values we have used Eq. (7).

Molecule	Carbon atom	σ Trimer	δ Trimer	Experimental δ values
g	C3	79.50	119.94	118.27
	C3a	72.59	124.82	125.51
	C4	141.22	49.66	47.22
	C5	160.36	28.70	28.66
	C6	153.11	36.64	35.73
	C7	140.19	50.79	49.45
	C7a	36.15	163.22	165.26
	C8	130.70	61.18	60.65
	7Me	175.79	11.81	12.45
	$8Me_{anti}$	169.00	19.24	20.26
	$8Me_{syn}$	168.08	20.25	22.15
h	C3	78.92	120.58	120.83
	C3a	71.72	125.76	125.51
	C4	142.12	48.68	47.22
	C5	159.11	30.07	29.57
	C6	155.20	34.35	33.00
	C7	139.03	52.07	50.41
	C7a	34.78	164.71	165.26
	C8	128.95	63.10	61.34
	7Me	176.18	11.38	10.57
	$8Me_{anti}$	169.50	18.70	17.56
	$8Me_{syn}$	168.44	19.86	20.84
i	C3	79.21	120.26	120.83
	C3a	73.07	124.29	125.51
	C4	141.46	49.40	47.22
	C5	160.28	28.79	28.66
	C6	154.48	35.14	34.98
	C7	139.23	51.84	50.41
	C7a	35.75	163.66	165.26
	C8	129.42	62.59	61.34
	7Me	175.95	11.64	11.64
	$8Me_{anti}$	169.00	19.25	20.26
	$8Me_{syn}$	168.98	19.26	20.84

4. Experimental

4.1. Chemistry

Compound **1** was prepared according to Jacquier and Maury [3]; the synthesis of the racemate, **1** + **2**, has already been described [33].

4.2. Crystal structure determination for (*1* + *2*) racemate

A summary of crystal data and refinement details are presented in Table 2 in comparison with information from the reported LABHEB structure. A data crystal was selected and mounted on a glass fiber using Paratone® oil flash-cooled to 120 K. Data were collected on a Bruker-AXS APEX CCD diffractometer with graphite-monochromated Mo-Kα radiation (λ = 0.71073 Å). Unit cell parameters were obtained from 60 data frames, 0.3° ω, from three different sections of the Ewald sphere. The systematic absences in the data and the unit cell parameters were consistent with $P2_1$ and $P2_1/m$. Intensity statistics and non-crystallographic information were consistent with the non-centrosymmetric space group option. The data-sets were treated with SADABS absorption corrections based on redundant multiscan data [34]. The structures were solved using direct methods and refined with full-matrix, least-squares procedures on F^2. The absence of heavy atoms precludes direct determination by anomalous dispersion, Friedel pairs were merged, and absolute configuration was assigned by non-crystallographic considerations. Six symmetry-independent molecules of the compound were located with one molecule enantiomerically disordered having a refined site ratio of 66/34. The molecules of the minor disordered component and those located at non-disordered sites are of the same chirality. The nitrogen atoms of the disordered molecule were constrained to have the same positions. The chemically equivalent non-hydrogen atoms in the disordered molecule were constrained to have the same anisotropic displacement parameters. The chemically equivalent 1,2 and 1,3 atomic separations in the disordered molecule were restrained to be the same within 0.02 standard deviations. All non-hydrogen atoms were refined with anisotropic displacement parameters. All hydrogen atoms were treated as idealized contributions. Atomic scattering factors are contained in the SHELXTL 6.12 program library [34]. The CIF has been deposited with the CCDC under deposition number **747613**.

4.3. NMR spectroscopy

Solution NMR spectra were recorded on a Bruker DRX 400 (9.4 Tesla, 400.13 MHz for ^1H and 100.62 MHz for ^{13}C) spectrometer with a 5-mm inverse-detection H–X probe equipped with a *z*-gradient coil, at 300 K. Chemical shifts (δ in ppm) are given from internal solvent, $CDCl_3$ 7.26 for ^1H and 77.0 for ^{13}C.

Solid state ^{13}C (100.73 MHz) and ^{15}N (40.60 MHz) CPMAS NMR spectra have been obtained on a Bruker WB 400 spectrometer at 300 K using a 4 mm DVT probehead. Samples were carefully packed in a 4-mm diameter cylindrical zirconia rotor with Kel-F end-caps. Operating conditions involved 3.2 μs 90° ^1H pulses and decoupling field strength of 78.1 kHz by TPPM sequence. ^{13}C spectra were originally referenced to a glycine sample and then the chemical shifts were recalculated to the Me_4Si [for the carbonyl atom δ(glycine) = 176.1 ppm] and ^{15}N spectra to $^{15}NH_4Cl$ and then converted to nitromethane scale using the relationship: δ ^{15}N ($MeNO_2$) = $\delta^{15}N(NH_4Cl)$–338.1 ppm. Typical acquisition parameters for ^{13}C CPMAS were: spectral width, 40 kHz; recycle delay, 5 s; acquisition time, 30 ms; contact time, 2 ms; and spin rate, 12 kHz. In order to distinguish protonated and unprotonated

carbon atoms, the NQS (Non-Quaternary Suppression) experiment by conventional cross-polarization was recorded [35]. Acquisition parameters for ^{15}N CPMAS were: spectral width, 40 kHz; recycle delay, 5 s; acquisition time, 35 ms; contact time, 6 ms; and spin rate, 6 kHz.

4.4. Differential scanning calorimetry

The DSC analyses were carried out using a Seiko DSC 220C connected to a Model SSC5200HDisk Station. Thermograms were recorded at the scanning rate of 5.0 °C min^{-1}.

4.5. Optical rotatory power

The specific rotation at 25° was determined with a Perkin Elmer model 241 polarimeter (sodium line, λ_{max} = 589 nm) using *ca.* 5 mg in 2 mL of $CHCl_3$.

4.6. Theoretical calculations

Theoretical calculations were carried out within the Gaussian 03 facilities [36]. The geometries were optimized at the B3LYP/6-31G(d) level [37,38], fully in the case of the isolated molecule (frequency calculations verified its minimum nature) used for solution studies or only the H atoms for the crystal molecules (not minima). On these geometries GIAO calculations [39] were carried out, GIAO/B3LYP/6-31G(d).

Acknowledgements

This work has been financed by the Spanish MEC (CTQ2007-62113 and CTQ2007-61901/BQU) and Comunidad Autónoma de Madrid (Project MADRISOLAR, ref. S-0505/PPQ/0225).

References

[1] O. Wallach, Liebigs Ann. Chem. 329 (1903) 82;
O. Wallach, A. Steindorff, Liebigs Ann. Chem. 329 (1903) 130.
[2] G.A. Nyman, G. Alfthan, Finska Kemist. Fest. J. (1944) 291;
G.A. Nyman, G. Alfthan, Chem. Abstr. 41 (1947) 6228.
[3] R. Jacquier, G. Maury, Bull. Soc. Chim. Fr. (1967) 295.
[4] S.I. Nagai, N. Oda, I. Ito, Yakugaku Zasshi 99 (1979) 705.
[5] A.A. Watson, D.A. House, P.J. Steel, J. Organomet. Chem. 311 (1986) 387.
[6] U. Groselj, D. Bevk, R. Jakse, S. Recnik, A. Meden, B. Stanovnik, J. Svete, Tetrahedron 61 (2005) 3991.
[7] A.L. Llamas-Saiz, C. Foces-Foces, I. Sobrados, J. Elguero, W. Meutermans, Acta Crystallogr. C 49C (1993) 724.
[8] A.A. Watson, D.A. House, P.J. Steel, Aust. J. Chem. 48 (1995) 1549.
[9] P. Cabildo, R.M. Claramunt, P. Cornago, J.L. Lavandera, D. Sanz, N. Jagerovic, M.L. Jimeno, J. Elguero, I. Gilles, J.L. Aubagnac, J. Chem. Soc. Perkin Trans. 2 (1996) 701.
[10] M. Barz, H. Glas, W.R. Thiel, Synthesis (1998) 1269.
[11] A.A. Watson, D.A. House, P.J. Steel, J. Org. Chem. 56 (1991) 4072.
[12] P.J. Steel, Molecules 8 (2004) 440.
[13] H. Brunner, T. Scheck, Chem. Ber. 125 (1992) 701.
[14] C.J. Tokar, P.B. Kettler, W.B. Tolman, Organometal 11 (1992) 2737.
[15] D.D. LeCloux, C.J. Tokar, M. Osawa, R.P. Houser, M.C. Keyes, W.B. Tolman, Organometal 13 (1994) 2855.
[16] B. Therrien, A. Konig, T.R. Ward, Organometal 18 (1999) 1565.
[17] M.C. Keyes, B.M. Chamberlain, S.A. Caltagirone, J.A. Halfen, W.B. Tolman, Organometal 17 (1998) 1984.
[18] J. Elflein, F. Platzmann, N. Burzlaff, Eur. J. Inorg. Chem. (2007) 5173.
[19] T. Godau, F. Platzmann, F.W. Heinemann, N. Burzlaff, Dalton Trans. (2009) 254.
[20] F.H. Cano, C. Foces-Foces, A.L. Llamas-Saiz, H.H. Limbach, F. Aguilar-Parrilla, R.M. Claramunt, C. López, J. Heterocycl. Chem. 31 (1994) 695.
[21] A. Martínez, M.L. Jimeno, J. Elguero, A. Fruchier, New J. Chem. 18 (1994) 269.
[22] CSD database version 5.30 (2008) Feb-09 and May-09 updates.;
F.H. Allen, W.D.S. Motherwell, Acta Crystallogr. B 58 (2002) 380;
F.H. Allen, W.D.S. Motherwell, Acta Crystallogr. B 58 (2002) 407.
[23] I. Alkorta, J. Elguero, Struc. Chem. 14 (2003) 377.
[24] A.E. Aliev, K.D.M. Harris, Probing Hydrogen Bonding in Solids Using Solid State NMR Spectroscopy, Structure & Bonding, Springer, Berlin/Heidelberg, 2004. p. 1.
[25] J.W. Steed, Cryst. Eng. Comm. 5 (2003) 169.
[26] Structures with $Z' > 4$. Z' website: http//www.dur.ac.uk/zprime.
[27] R. Bishop, M.L. Scudder, Cryst. Growth Des. 9 (2009) 2890.
[28] C. Foces-Foces, I. Alkorta, J. Elguero, Acta Crystallogr. B B56 (2000) 1018.
[29] I. Alkorta, J. Elguero, C. Foces-Foces, L. Infantes, Arkivoc ii (2006) 15.
[30] O. Prakash, A. Kumar, A. Sadana, R. Prakash, S.P. Singh, R.M. Claramunt, D. Sanz, I. Alkorta, J. Elguero, Tetrahedron 61 (2005) 6642.
[31] R.K. Harris, S.A. Joyce, C.J. Pickard, S. Cadars, L. Emsley, Phys. Chem. Chem. Phys. 8 (2006) 137.
[32] F. Doro, P. Bailey, S. Parsons, Private Communication to CCDC from School of Chemistry, The University of Edinburgh, Edinburgh, Scotland, EH9 3JJ, United Kingdom, 2007.
[33] R.M. Claramunt, C. López, C. Pérez-Medina, M. Pérez-Torralba, J. Elguero, G. Escames, D. Acuña-Castroviejo, Bioorg. Med. Chem. 17 (2009) 6180.
[34] G.M. Sheldrick, Acta Crystallogr. A A64 (2008) 112.
[35] S. Berger, S. Braun, "200 and More NMR Experiments, Wiley-VCH, Weinheim, 2004.
[36] M.J. Frisch, G.W. Trucks, H.B. Schlegel, G.E. Scuseria, M.A. Robb, J.R. Cheeseman, J.A. Montgomery Jr., T. Vreven, K.N. Kudin, J.C. Burant, J.M. Millam, S.S. Iyengar, J. Tomasi, V. Barone, B. Mennucci, M. Cossi, G. Scalmani, N. Rega, G.A. Petersson, H. Nakatsuji, M. Hada, M. Ehara, K. Toyota, R. Fukuda, J. Hasegawa, M. Ishida, T. Nakajima, Y. Honda, O. Kitao, H. Nakai, M. Klene, X. Li, J.E. Knox, H.P. Hratchian, J.B. Cross, C. Adamo, J. Jaramillo, R. Gomperts, R.E. Stratmann, O. Yazyev, A.J. Austin, R. Cammi, C. Pomelli, J.W. Ochterski, P.Y. Ayala, K. Morokuma, G.A. Voth, P. Salvador, J.J. Dannenberg, V.G. Zakrzewski, S. Dapprich, A.D. Daniels, M.C. Strain, O. Farkas, D.K. Malick, A.D. Rabuck, K. Raghavachari, J.B. Foresman, J.V. Ortiz, Q. Cui, A.G. Baboul, S. Clifford, J. Cioslowski, B.B. Stefanov, G. Liu, A. Liashenko, P. Piskorz, I. Komaromi, R.L. Martin, D.J. Fox, T. Keith, M.A. Al-Laham, C.Y. Peng, A. Nanayakkara, M. Challacombe, P.M.W. Gill, B. Johnson, W. Chen, M.W. Wong, C. Gonzalez, J.A. Pople, Gaussian 03, Gaussian, Inc., Pittsburgh PA, 2003.
[37] A.D. Becke, Phys. Rev. A 38 (1988) 3098;
A.D. Becke, J. Chem. Phys. 98 (1993) 5648;
C. Lee, W. Yang, R.G. Parr, Phys. Rev. B 37 (1988) 785.
[38] P.A. Hariharan, J.A. Pople, Theor. Chim. Acta 28 (1973) 213.
[39] R. Ditchfield, Mol. Phys. 27 (1974) 789;
F. London, J. Phys. Rad. 8 (1937) 397.